Journal of Metals, Materials and Minerals. Vol. 12 No. 2 pp. 51-57, 2003.

The Application of Electron Channeling Contrast Mode to Study the Recrystallization Process in Nickel Alloy after Different Thermomechanical Processing Conditions

Panyawat WANGYAO[1], Jozef ZRNIK[2], Josef KASL[3], Zbysek NOVY[4] and Piyamanee KOMOLWIT[5]

[1]Metallurgy and Materials Science Research Institute, Chulalongkorn University, Bangkok, Thailand
[2]Materials Science Dept., Faculty of Metallurgy, Technical University, Košice, Slovakia
[3]Materials and Technology Research, Škoda Research Institute, Plzeň, Czech Rep.
[4]Complete Technological Service-Forming & Heat Treatment s.r.o., Plzeň, Czech Rep.
[5]Materials Science and Engineering Dept., School of Engineering, San Jose State University, U.S.A.

ABSTRACT

This paper describes the effect of different thermomechanical processing (TMP) conditions on the evolution of the recrystallized structure of NiMoCr alloy. The hot working conditions and various heat treatment parameters were employed in order to influence the recrystallization process of the alloy. The changes in microstructure resulting from tested programs were investigated by a scanning electron microscope in electron channeling contrast mode. By applying this method, it was possible to detect and evaluate the difference between deformed and recrystallized grains in the microstructures. The results showed that the uniformity and the percentage amount of recrystallized area increases when a longer annealing time and/or higher amount of deformation during TMP were employed.

INTRODUCTION

The solid solution of nickel based alloy, NiMoCr, an experimental material, has applications in the frame of the development of an *Accelerated Driven Transmission Technology* loop (ADTT) for a molten salt-type nuclear reactor (Hosnedl, *et al*. 1998). This work intended to study the effect of static recrystallization on the microstructure development after thermomechniacal processing and annealing processes. SEM with *electron channeling contrast mode (ECCM)* was employed to detect the differences between deformed grains (distorted orientation in grains) and perfect grains (recrystallized structure), which would be difficult when only polarized microscopy could be used.

ECCM technique, which was employed in this study, can be briefly described as follows. The electron channeling effect arises because of the differing atomic packing density, which is observed along different crystallographic directions. When the primary electron beam hit the sample surface Figure 1A, where the atomic

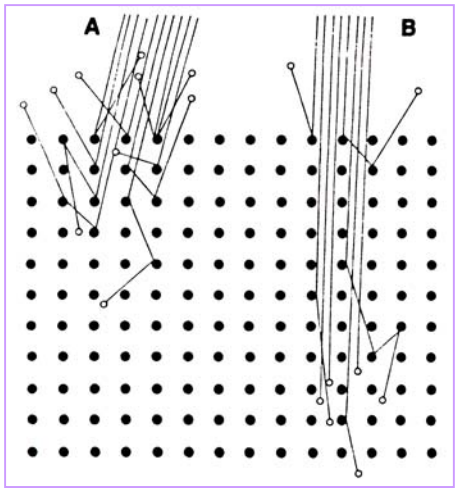

Figure 1. Schematic representation of a crystal lattice. Two different beam-crystal orientations are indicated demonstrating (A) a non-channeling and (B) A channeling situation (Newbury, *et al*. 1986).

packing is high, electrons are reflected close to the surface. When the electron beam has a slightly different angle, relative to the crystal structure, it penetrates more deeply into the crystal, passing between the rows of atoms along "channels", before hitting the crystal structure inside Figure 1B. The presence of defects in the structure such as dislocation (distorted lattice) has an effect on divergence of the beam (Newbury, *et al*. 1986; Robertson; and Evangelista *et al.* 1993). Therefore, the wavy channeling pattern is possibly observed with distinct bands.

Material and Experimental Procedure

The chemical composition of NiMoCr sample in wt. % is shown in Table 1. The sample was prepared in 3 steps: casting, multi-step forging and annealing. The ingot sample from the casting process then was broken down by multi-step forging. However, the samples were not a fully uniform structure as desired. Therefore, the shape reduction technique was employed to get a more uniform structure for the final sheet product. Then various deformation schedules were modified and applied from previous works (Novy, *et al*. 1999; and Novy, *et al.* 1998) to optimize thermomechanical-processing conditions securing the uniform recrystallized structure. The employed TMP condition consisted of a hot working and cooling process, followed by an annealing processes, as shown in Table 2. Then, the specimen was electropolished and investigated by image analysis via SEM.

Table 1 Chemical composition of NiMoCr alloy.

Ni	Mo	Cr	Fe	Al	Ti	W	Co	Si	Cu	B	S	C
72.7	17.8	6.3	2.8	0.16	0.06	0.06	0.06	0.05	0.01	0.01	0.001	0.02

Table 2 Details of hot working and cooling conditions.

Specimen No.	Heating temperature before hot working (ºC)	% reduction during hot working	Annealing time (min) at 1,100 ºC
A1	1,200 ºC/30 min	18%+18%	Quenching
A2	1,200 ºC/30 min	18%+18%	Air cooling
A3	1,200 ºC/30 min	18%+18%	3 min
A4	1,200 ºC/30 min	18%+18%	5 min
A5	1,200 ºC/30 min	18%+18%	10 min
A6	1,200 ºC/30 min	18%+18%	15 min
A7	1,200 ºC/30 min	18%+18%	25 min
A8	1,200 ºC/30 min	18%+18%	50 min
B1	1,100 ºC/30 min	11.3%+13.6%	Quenching
B2	1,100 ºC/30 min	11.3%+13.6%	3 min
B3	1,100 ºC/30 min	11.3%+13.6%	5 min
B4	1,100 ºC/30 min	11.3%+13.6%	10 min
B5	1,100 ºC/30 min	11.3%+13.6%	25 min
B6	1,100 ºC/30 min	11.3%+13.6%	50 min

RESULTS AND DISCUSSION

Microstructural analysis by SEM and image analyser

The backscattered electron mode of SEM was employed under ECC conditions for recrystallization structure analysis and provide fine detail of structure evolution in the early stages of the recrystallization. The specimens were electrolytically polished after the thermomechanical processes of the NiMoCr alloy had been investigated by the above method. For both programs, A and B, in specimens that were cooled by water (quenching) and air (air-cooling) immediately after the hot working process, it was found that in all observed sections the

microstructure appeared to have completely deformed features, as illustrated in Figure 2 and Figure 3. Only the SEM using ECC mode could reveal these fully complex bend contours. The result indicated the evidence that static recrystallization does not occur during and/or after hot deformation. This was consistent with results from previous work Wangyao, (2002), which deformed substructure was investigated by TEM and it was found that the deformed substructure had very dense dislocations.

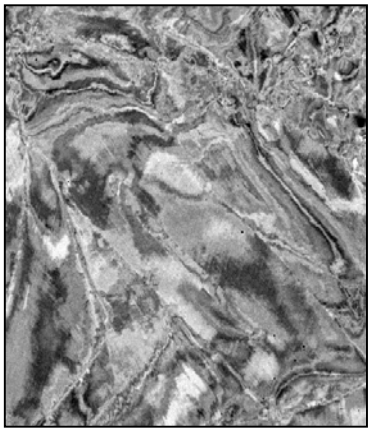

Figure 2 Fully deformed microstructure after quenching, 200X.

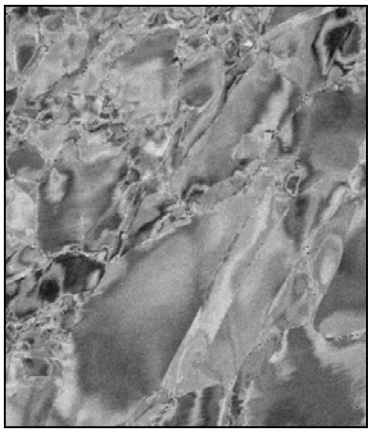

Figure 3 Small dynamically recrystallized grains around primary coarse grains after quenching, 200X.

Structure analysis results, on one side, show that if dynamic recrystallization occurred, it would be to a very small extent. In addition, in these grains there would be the presence of the residual dislocation substructure. The statement agreed with TEM results as proven by previous work (Wangyao, 2002). When considering the grain structure in Figure 3, it should be noted that the fine dynamically recrystallized grains occurred around the primary coarse grains and were simultaneously deformed during the hot working process, as found in results of previous work (Novy, *et al*. 1999). Thus, this SEM analysis could not properly detect the dynamic recrystallization due to the fact that the structure was yet subjected to hot deformation and bears the features of strain presence. The forming process of fast and air-cooling was carried out just to investigate and confirm if any recrystallization would occur.

The progress of static recrystrallization during the annealing process in various steps is presented via specimens (No. A3-A8 and B2-B6) in cross-sections and parallel to the longitudinal axis. The advancement of the static recrystallization process is dependent on the time of annealing as shown in Figures 4-7, for various annealing times. Primarily, the fine statically recrystallized grains formed along the coarse deformed grain boundaries after 3 minutes of annealing as can be seen in Figure 4. This result was confirmed by ECC analysis. Annealing twins also appeared in fine static recrystallized grains. Therefore, these statically recrystallized grains could possibly originate mainly in 3 regions; 1) along the primary coarse grain boundaries, 2) inside coarse primary grains, and 3) around the coarse primary grains developing from previous fine dynamically grains.

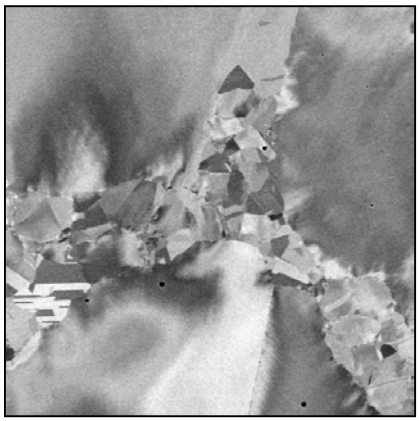

Figure 4 Very fine statically recrystallized grains were generated among the primary coarse grain boundaries, 400X.

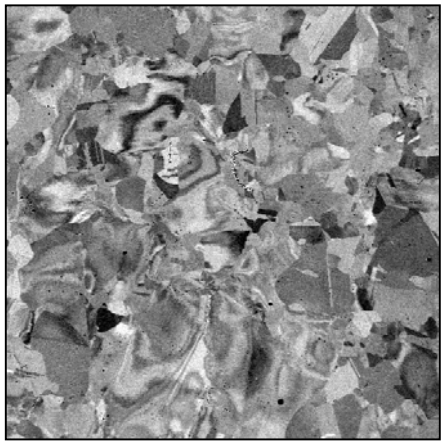

Figure 5 Mixed microstructures between still deformed and recrystallized grains after 5 minutes annealing, Specimen No. A3, 200X.

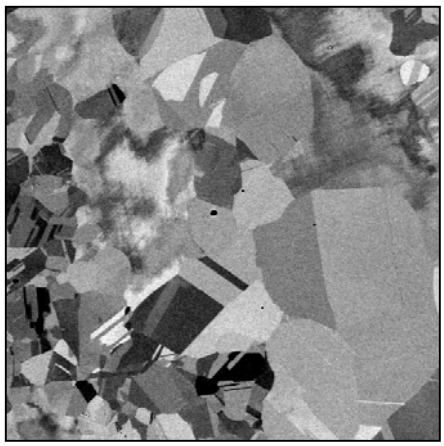

Figure 6 Mixed microstructures after 10 minutes annealing, Specimen No. B4, 200X.

However, after 50 minutes of annealing the presence of deformed grains to a small extent was still possibly observed in the microstructure. As annealing time increased, it can be seen that the fine statically recrystallized grains (in short annealing time) became coarser and more uniform, as illustrated in Diagram 1. This grain coarsening should be the result of successive secondary recrystallization processes, which is not extensive. The progressive results of static recrystallization observed by the ECC mode for this alloy gradually developed as annealing time passed. Diagram 1 shows that the amount of % recrystallization increased as annealing time increased.

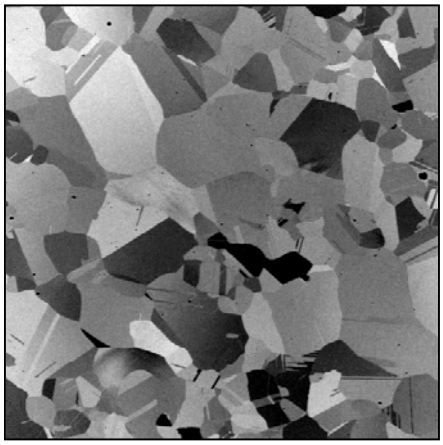

Figure 7 A small amount of deformed structure was still observed after 50 minutes annealing (lower left), Specimen No. A7, 200X.

To summarize the results, the microstructure after TMP and annealing process of the alloy shows a mixture of recovered (in small portions) and mostly recrystallized structure. The critical time for annealing when most of the structure was being recrystallized, appeared to be 10 minutes of annealing, independent of the deformation temperature. However, for all cases of TMP, it was also found that the amount of detected static recrystallization in the structure close to the surface was much lower than those in other interior areas. This was probably due to the lower surface temperature by atmosphere of air-cooling, which had an effect on slowing the progress of recrystallization. Furthermore, the specimen surface could also lose heat by touching with the tool face (heat transfer) and hindering the recrystallization process. Therefore, only small amounts of static recrystallization could take place.

Another possible reason, which caused the static recrystallization process to slow down could be due to that stored energy was almost already consumed to generate very fine dynamic recrystallized grains at the surface during hot rolling. This area of the specimen was subjected to a higher strain concentration than the interior of the specimen during forming. Thus, during the next step annealing, the remaining stored energy in surface areas provided a lower diving force to generate static recrystallization, which then had been taking place in lower amounts compared to the interior during annealing.

55

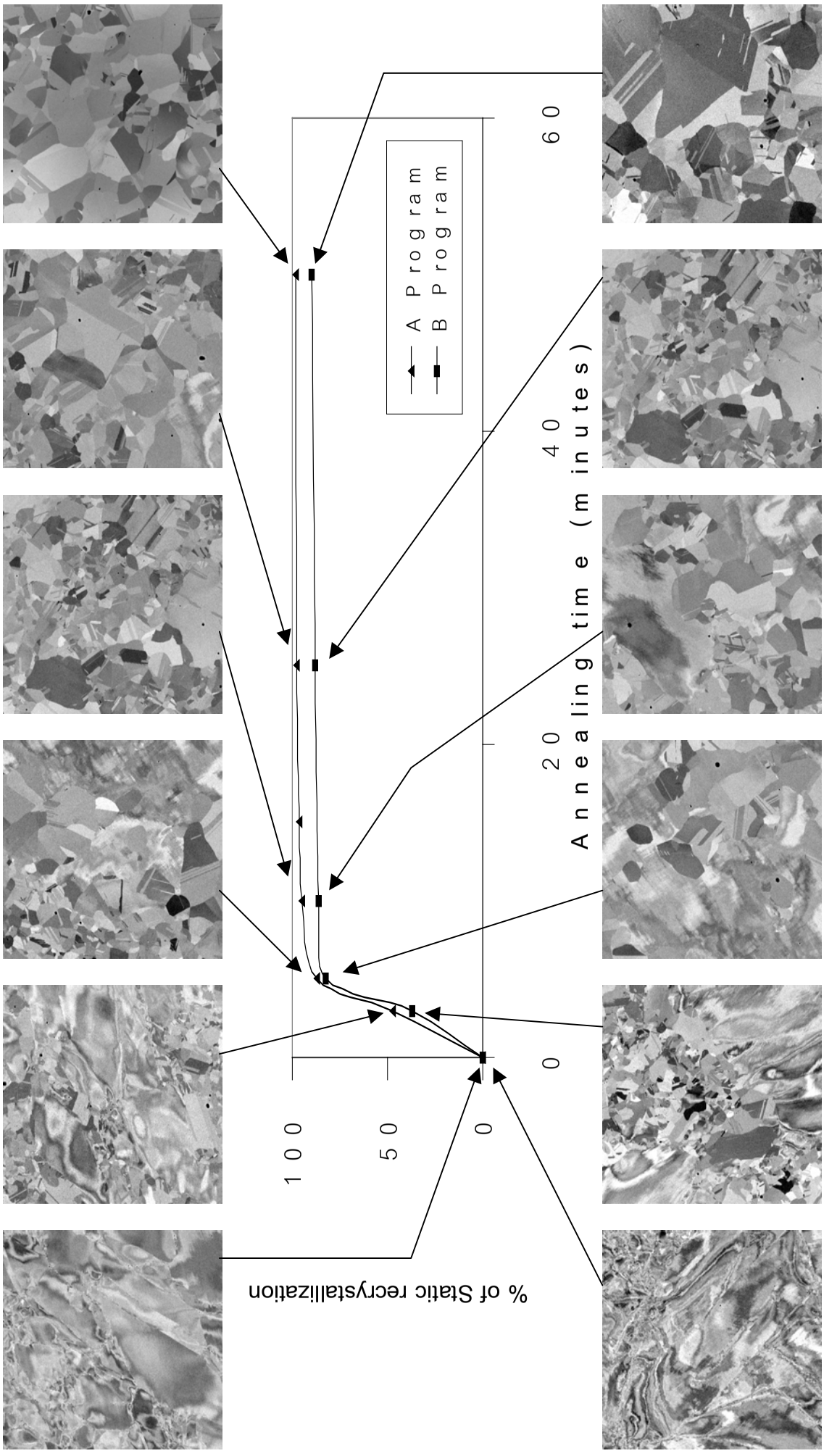

Diagram 1 The relationship between % static recrystallization and annealing time (minutes).

To compare recrystallization progress from both TMP programs, with respect to recrystallization progress, the amount of static recrystallization in program A was slightly higher than that in program B. This could imply that the specimens which proceed according to program A, received more stored energy from a higher amount of deformation introduced during the hot working process than those in program B. The difference in TMP conditions resulted in different final amounts of recrystallized structure. Specimens from program A had a total amount of static recrystallization of nearly 100% (in 50 minutes of annealing time), while it was closely 90% of the specimens from program B. This difference can be explained by an effect of a higher amount of stored energy in the microstructure of program A providing faster static recrystallization. However, it should be noted that in both programs, the observed and measured amount of % static recrystallization portion was already high, approximately about 90% after annealing for 10 minutes.

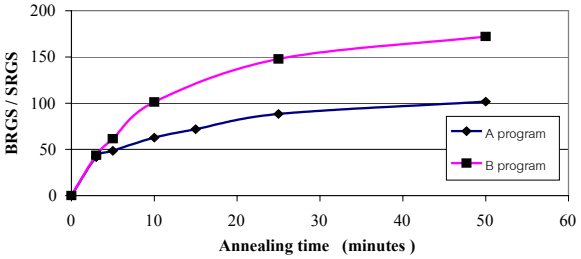

Figure 8 The relationship between BRGA/ SRGA and annealing time.

To evaluate the recrystallization results, Figure 8 demonstrates the recrystallizion and grain growth behavior. The average biggest recrystallized grain area per the average smallest recrystallized grain area (BRGA/SRGA), obtained from measured and calculated data of ECC images, increased as annealing time increased. The growth of recrystallized grain increased rapidly at the beginning of the period up to 10 minutes as a result of a higher driving force accumulated due to stored energy. As the annealing time prolonged then the dependence continued slowly in increasing as a result of lower driving force from the decrease in surface energy. It should be noted that the values of SRGA in all cases were received as the same value, which could be detected in the recrystallized structure by an image analyzer after the beginning of the process for the shortest annealing time.

To follow the results of all programs, it was found that after the annealing process within the frame time of experiments, all observed annealed microstructures were almost completely recrystallized (which were close to 100 % static recrystallization), see Diagram 1. However, such nearly complete recrystallization behavior should be caused by the heterogeneous nature of previous dynamic substructures (Sakai, 1995). When hot deformation was ceased, the dynamic recrystallization (DRX) nuclei might continue to grow, leading to metadynamic recrystallization (MDRX) in their localities. The growing DRX grains should contain few dislocations near their boundaries, and then classical nucleation was not possible to occur within them. Accordingly, they could only be softened by metadynamic recovery (MDRV) in their interiors. Finally, the full work hardened DRX grains were recovered statically under the annealing process then underwent static recrystallization (SRX). However, the incomplete softening could be caused by the stable existence of growing DRX grains having many-sided irregular shapes with high-density dislocations, therefore, with further annealing of such mixed microstructures (i.e., MDRX or SRX new grains and MDRV grains containing the moderate dislocation densities). Hence, the growth rate of new recrystallized grains should decrease because of a small difference in dislocation densities across their boundary (Xu and Sakai, 1991).

CONCLUSION

The annealing process, which followed the hot-working process, caused the static recrystallization to occur consequently, the heterogeneity in the microstructure decreased as annealing time increased. The recrystallization occurred during a longer annealing time a providing more uniform grain structure. Microstructures according to program A were more uniform than those from program B. Due to the degree of deformation during hot working had strongly influencesd the final grain structure (size and morphology), the greater the degree of deformation, the finer the recrystallized grain size was obtained.

REFERENCES

Hosnedl, P., Vaclav, V. and Novy, Z. 1998. *Development of corrosion resistance alloy MoNiCr for molten fluoride salts (recrystallization of MoNiCr alloy),* Škoda vyzkum report. : 1-10.

Newbury, D. E., Joy, D. C., Echlin, P., Fiori, C.E. and Goldstein, J. I. 1986. *Electron channeling contrast in the SEM, in Advanced Scanning Electron Microscopy and X-ray Microanalysis*. Plenum Press.

Robertson, V. E. *Introduction to the principle of operation and applications of the scanning electron microscope and electron microprobe.* Technical information from JEOL Company, U.S.A.

Evangelista, E., Mengucci, P., Bowles, J., and McQueen, H. J. 1993. Grain and subgrain structure developed by hot working in As-cast 434 stainless steel. *High Temp. Mater. and Processes*. **12** : 57-65.

Nový, Z., Zrnik, J., Nemecek, S., and Kasl, J. 1999. The influence of deformation condition on recrystallization behaviour of NiMoCr alloy. *Physical Metallurgy and Fracture of Materials.* 99 : 151-155.

Nový, Z. Nemecek, S. and Kasl, J. 1998. *Recrystallization of NiMoCr alloy, Škoda vyzkum report*. : 1-12.

Wangyao, P. 2002. *Optimalising of the formability and high temperature properties of nickel base superalloy pre-determined for nuclear reactor.* Doctoral. Dissertation, Technical University of Košice. : 83-89.

Nový, Z., Kraus, L., Kasl, J., Nemacek, S., Fiala, J., Sindler, I., and Zrnik, J. 1999. Recrystallization of NiMoCr alloy. *Acta Metallurgica Slovaca*. **5**: 274-278.

Sakai, T. 1995. Dynamic recrystallization microstructure under hot working conditions. *Advance Materials & Technologies*. : 381-384.

Xu, Z. and Sakai, T. 1991. *Journal of Japanese Institute of Metals.* **55** : 1298.

(Revised version accepted March 17, 2003)